Fractional Fokker–Planck equation approach for the interconversion between dielectric and mechanical measurements

A. Garcia-Bernabé,[1,a)] M. J. Sanchis,[1] R. Díaz-Calleja,[1] and L. F. del Castillo[2]
[1]*Departamento de Termodinámica Aplicada and Instituto de Tecnología Eléctrica, Universidad Politécnica de Valencia, 46022 Valencia, Spain*
[2]*Instituto de Investigaciones en Materiales, Universidad Nacional Autónoma de México, Ap. Postal 70-360, Coyoacán, México DF 04510, Mexico*

(Received 27 April 2009; accepted 30 May 2009; published online 14 July 2009)

This work describes a model of interconversion between mechanical and dielectric measurement. A previous version of this model has been proposed in the hereafter called "previous paper" [Díaz-Calleja, *et al.*Phys. Rev. E **72**, 051505 (2005)], starting from a scaling relation between the translational and rotational viscosities present in a glass forming liquid near the glass transition temperature. Now, in order to improve the previous procedure, the following modifications have been made: (1) a definition of the rotational viscosity obtained from a fractional Fokker–Planck equation has been used, (2) the complex translational viscosity is taken as a non-Newtonian one, (3) a careful splitting of α and β relaxations is necessary, because the interconversión algorithm depends on the underlying molecular mechanism of each relaxation, and (4) the modulus and phase angle of complex viscosities were analyzed instead of real and imaginary parts of the complex viscosities. The proposed interconversion model, in the interval of frequencies 10^{-2}–10^{+5} Hz, shows that the obtained results are more accurate than those one obtained in the previous paper.
 [DOI: 10.1063/1.3158555]

I. INTRODUCTION

The background analysis of the present paper is given by the contribution made by the DiMarzio–Bishop (DMB) approach, which expresses the Debye rotational frictional coefficient of a dipole in terms of the complex shear viscosity.[1,2] This contribution gives a generalization of the Debye theory to include memory effect on the basic assumption that the total dielectric memory effect is produced by stress relaxation.

The results obtained by using the DMB equation are only in qualitative agreement with experimental data but they still describe some details of the interconversion between the dielectric and mechanical measurements.[3–5] To overcome this drawback of the theory, a one-dimensional fractional Fokker–Plank (FFP) equation has been used to extend the classical Debye theory[6] to obtain a more flexible Cole–Cole equation.[7–9]

The appearance of a FFP equation, that we will call Smoluchowski equation in the present context, is based on the concept of a generalized version of the continuous time random walk (CTRW) to include the effect of the time dependent jump probabilities.[10,11] Systems at which CTRW is applied exhibit anomalous diffusion, that is, diffusion in disordered fractal structures or, more specifically, fractal time random walks.[12]

A simple case of CTRW arises when one assumes that the jump length and the jump time random variables are decoupled. The jump length distribution becomes Gaussian in the limit, while the mean waiting time between jumps diverges. Such walks, possessing a discrete hierarchy of time scales as known as fractal time random walks. In the limit of a large sequence of jump times, they give rise to a fractional diffusion equation or FFP equation in the configuration space and, as a consequence, to anomalous relaxation behavior.

The CTRW model is appropriate to describe a broad set of physical phenomena related to the physics of condensed matter. In particular, it should be noted that CTRW has been used by Dyre to describe the low frequency conduction in polymers.[13]

In a previous paper[14] a comparison between these data for the ester dicyclohexyl methyl-2-methyl succinate (DCMMS) were carried out. From the experimental point of view, the analysis was carried out on the assumption that only one relaxation was present in the experimental data. Nevertheless, a careful analysis of the dynamic mechanical as well as dielectric data obtained from the polymers derived from this compound show the presence of a prominent β relaxation.[15–17] The DCMMS has many degrees of freedom in the chain giving rise to many possible molecular conformations, which are the origin of a particularly complex dielectric as well as mechanical relaxation spectra. For this reason, we considered pertinent a careful characterization of the experimental dielectric and mechanical data in order to analyze in a separated form the alpha and beta relaxations.

Another prescription that was used in the previous paper[14] is based on the decoupling of the rotational diffusion and shear viscosity.[18] The equality was accounted in the Debye–Stokes–Einstein (DSE) relation for the rotational diffusion coefficient. Now it is allowed to be different from each other, or partially related, which implies that the rotational diffusion coefficient scales with the shear viscosity as a power law with an exponent ranging between zero and

a)Electronic mail: agarciab@ter.upv.es.

one.[19,20] This value reflects the degree of coupling between the mechanical and dielectric relaxation mechanisms.

In the present paper the problem has been revisited on grounds to confirm the aforementioned assumption. The plan of the paper is as follows. In Sec. II A we propose a modification of the DMB equation[1] based on the use of a FFP equation. This procedure allows us to obtain a Cole–Cole-like equation where a fractional power rotational viscosity appears in a natural way. In Sec. II B, a fractional power law for the relationship between the shear viscosity and the shear modulus has been proposed. In fact the departure of the Newtonian behavior for the viscous fluid is used considering a power law.[21,22] In Sec. II C, a relation between complex rotational and translational viscosities as complex magnitudes has been proposed. In Secs. III A and III B, we ensure that we are in the presence of an isolated α relaxation to be subsequently analyzed. In Sec. IV, we discuss the validity of the interconversion algorithm.

II. INTERCONVERSION MODEL FOR ALPHA RELAXATION

A. Rotational viscosity

The one dimensional FFP can be written as[8]

$$\frac{\partial}{\partial t}f(x,t) = {}_0D_t^{1-a}K_a\frac{\partial^2}{\partial x^2}f(x,t), \tag{1}$$

where the Riemann–Liouville operator ${}_0D_t^{1-a}=[\partial/\partial t]{}_0D_t^{-a}$ is defined through the relation[23]

$${}_0D_t^{1-a}f(x,t) = \frac{1}{\Gamma(a)}\frac{\partial}{\partial t}\int_0^t dt'\frac{f(x,t')}{(t-t')^{1-a}}. \tag{2}$$

The generalized (or fractional) diffusion coefficient K_a appearing in Eq. (1) is defined by

$$K_a \equiv \sigma^2\tau^{-a}, \tag{3}$$

where σ^2 is the mean squared displacement, τ is the relaxation time, and $[K_a]$ has the dimension $\mathrm{cm}^2\ \mathrm{s}^{-a}$.

On these grounds the Debye–Smoluchowski equation for the rotational diffusion of dipoles can be written as

$$\frac{\partial f}{\partial t} = {}_0D_t^{1-a}\frac{1}{\sin\theta}\frac{\partial}{\partial\theta}\left[\sin\theta\left(K_a\frac{\partial f}{\partial\theta} - M\frac{f}{\xi_a}\right)\right], \tag{4}$$

where ξ_a is a rotational generalized friction coefficient with the dimension $[\xi_a]=s^{a-2}$ and $K_a=k_BT/m\xi_a$ is the generalized DSE relation.

Then, according to the DMB methodology,[1] Eq. (4) can be generalized to include memory effects for K_a, as well as for ξ_a, to

$$\frac{\partial f}{\partial t} = {}_0D_t^{1-a}\frac{1}{\sin\theta}\frac{\partial}{\partial\theta}\left[\sin\theta\left(\frac{\partial}{\partial\theta}\int_{-\infty}^t K_a(t-t')f(\theta,t')dt' - \frac{f}{k_BT}\int_{-\infty}^t K_a(t-t')M(t')dt'\right)\right], \tag{5}$$

where we used a generalized version of the DSE relation to express ξ_a in terms of K_a as DMB did [their Eqs. (II.7) and (II.13)].

To obtain the response to a sinusoidal electric internal field,

$$F = F\exp(i\omega t). \tag{6}$$

The torque due to this field will be given by

$$M = -\mu F\sin\theta, \tag{7}$$

where μ is the dipole moment of the rotating particle.

Now, following Debye, we assume a solution for Eq. (5) with the following form:

$$f = \frac{1}{2\pi}\left(1 + B(t)\frac{\mu F_0}{k_BT}\exp(i\omega t)\cos\theta\right). \tag{8}$$

By taking the Laplace transform of Eq. (5) by using Eqs. (6)–(8) and noting that

$$\boldsymbol{L}\left|{}_0D_t^{1-a}f(t)\right| = s^{1-a}f(s) - D_t^{-a}f(t)\big|_{t=0}, \tag{9}$$

where $s=i\omega$; the following result is obtained,

$$B(\omega) = \frac{1}{1+[i\omega\tau(\omega)]^a}, \tag{10}$$

where we used the following definition for the complex Debye relaxation time,

$$\tau^a(\omega) = \frac{1}{2K_a(\omega)} = \frac{m\xi_a(\omega)}{2k_BT}, \tag{11}$$

which is a generalization of Eq. (II.20a) of the DMB paper.[1]

Finally following the main lines of the Debye calculation for the complex dielectric permittivity, one obtains

$$\frac{\varepsilon^*(\omega)-\varepsilon_\infty}{\varepsilon_0-\varepsilon_\infty} = \frac{1}{1+\dfrac{\varepsilon_0+2}{\varepsilon_{\infty+2}}[i\omega\tau(\omega)]^a} = \frac{1}{1+\left[i\omega\tau(\omega)\left(\dfrac{\varepsilon_0+2}{\varepsilon_\infty+2}\right)^{1/a}\right]^a}, \tag{12}$$

which is a Cole–Cole type equation. Cole–Cole equation was introduced on empirical grounds to give account of the "anomalous" dispersion behavior observed in some polar liquids. In fact, it is equivalent to substitute the resistor in a parallel capacitance-(capacitance-resistor) passive electric circuit by a constant phase element (CPE).

The origin of this CPE can be found in a seminal paper of Cole–Cole.[24] In this paper, Cole changes an electrical resistor, which in the mechanical analogy corresponds to a pure viscosity into complex impedance that is to a CPE in electrical terms.[25] In the mechanical analogy this corresponds to a fractional complex viscosity. This assumption allows these authors to fit better the experimental results. We use a CPE in the DMB model in the same sense that Cole–Cole did.

Therefore, the generalized rotational viscosity $[\eta^*_{\mathrm{rot}}(\omega)]$ could be defined in terms of the following relation:

$$\frac{\varepsilon^*(\omega)-\varepsilon_\infty}{\varepsilon_0-\varepsilon_\infty} = \frac{1}{1+[i\omega A\,\eta^*_{\mathrm{rot}}(\omega)]^a}, \tag{13}$$

And, consequently,

$$A\,\eta^*_{\mathrm{rot}}(\omega)=\frac{1}{(i\omega)}\left(\frac{\varepsilon_0-\varepsilon_\infty}{\varepsilon^*(\omega)-\varepsilon_\infty}-1\right)^{1/a}, \tag{14}$$

where $A=(8\pi R^3/2k_BT)(\varepsilon_0+2/\varepsilon_\infty+2)^{1/a}$ and the a parameter should be chosen in such a way that the real and imaginary parts of the rotational viscosity do not show any divergence. That is, they have the same behavior than an experimental modulus. In fact, the real part shows a plateau at low frequency and the decreasing at high frequency, whereas the imaginary part shows a bell shape.

This generalized rotational viscosity will be expressed, as usual, as a function of the real and imaginary parts, as $\eta^*_{\mathrm{rot}}(\omega)=\eta'_{\mathrm{rot}}(\omega)-i\,\eta''_{\mathrm{rot}}(\omega)$, or, in terms of modulus and phase angle the rotational viscosity, as $\eta^*_{\mathrm{rot}}(\omega)=|\eta^*_{\mathrm{rot}}(\omega)|e^{i\varphi_{\mathrm{rot}}(\omega)}$.

B. Translational viscosity

The mechanical modulus usually is defined in the classical viscoelasticity theory by

$$G(t)-G(t=\infty)=\frac{d\eta(t)}{dt}. \tag{15}$$

By taking the Laplace transform of Eq. (15), the following result is obtained:

$$G(\omega)-G(0)=i\omega\eta^*(\omega). \tag{16}$$

In the same way as the previous section, the mechanical modulus can be related to the viscosity by means of the fractional time derivate as follows:

$$G(t)-G(t=\infty)=\frac{d^c\eta(t)}{dt^c}. \tag{17}$$

By taking the Laplace transform of this equation, the mechanical modulus can be expressed by

$$G^*(\omega)-G_0=(i\omega)^c\,\eta^*_{\mathrm{trans}}(\omega), \tag{18}$$

where $\eta^*_{\mathrm{trans}}(\omega)$ is the generalized translational viscosity, which has the dimension [Pa s^c] and c is a parameter, which plays the same role than parameter a in Eq. (13).

For computational purposes, the real and imaginary parts of the dynamic shear viscosity are given in terms of the frequency in a similar way as Eqs. (15) and (16).

$$\eta^*_{\mathrm{trans}}(\omega)=\eta'_{\mathrm{trans}}(\omega)-i\,\eta''_{\mathrm{trans}}(\omega)=|\eta^*_{\mathrm{trans}}(\omega)|e^{i\varphi_{\mathrm{trans}}(\omega)}. \tag{19}$$

C. Model for the relationship between both viscosities

In order to introduce a scale relationship between rotational and translational viscosities, we consider that the diffusion of a tracer particle is related to the shear viscosity according to the DSE relation. This equality is adequate for spherical particles of any radius rotating in a Newtonian fluid. However, for dipoles of the same size of the molecular fluid or dipoles in a viscoelastic fluid, as it is in the case of a supercooled liquid under nonergodic conditions, this result is for the DSE relation breakdown. This effect has been recognized as the decoupling of translational diffusion and the rotational motion of dipoles in dielectric relaxation, as a consequence of the dynamic heterogeneity.[18,26] Therefore, this decoupling modifies the DSE relationship and the equality of the rotational and translational viscosities. In this case, the relation between them can be formulated in terms of a power law with a fractional exponent, being this relationship valid not only for static, but also for the dynamic case, that is

$$\eta^*_{\mathrm{rot}}(\omega)=B[\eta^*_{\mathrm{trans}}(\omega\delta)]^\xi, \tag{20}$$

where B is a scale factor, ξ is a shape factor, and δ is a parameter that represents the shift of the curves in the frequency domain. These three parameters will be obtained by the fit of Eq. (20) to experimental data.

Furthermore, taking into account Eq. (20), the relationship between the modulus and phase angle of rotational and translational viscosities can be written as follows:

$$|\eta^*_{\mathrm{rot}}(\omega)|=B(|\eta^*_{\mathrm{trans}}(\omega\delta)|)^\xi, \tag{21}$$

$$\varphi_{\mathrm{rot}}(\omega)=\xi\varphi_{\mathrm{trans}}(\omega\delta). \tag{22}$$

These two equations will be used to relate the dielectric and mechanical experimental measurements. The interconversion between the dielectric and mechanical measurements can be carried out when the three fitting parameters involved in the proposed model (B, ξ, and δ) have been evaluated.

D. Evaluation of the dielectric permittivity from shear modulus and shear modulus from dielectric permittivity

According to the interconversion model, Eq. (20), and taking into account the α viscosities given in Eqs. (14) and (19), the α dielectric permittivity could be evaluated from α shear modulus as

$$\frac{\varepsilon^*(\omega)-\varepsilon_\infty}{\varepsilon_0-\varepsilon_\infty}=\frac{1}{1+\left(\frac{B'}{\delta^c}\right)^{\xi a}(i\omega)^{(1-c\xi)a}(G^*_s(\omega\delta)-G_0)^{\xi a}}, \tag{23}$$

where B' is $[B/A]$. Just like in the previous case, the α shear modulus should be determined from the α dielectric permittivity as

$$G^*_s(\omega\delta)-G_0=\left[\frac{\varepsilon_0-\varepsilon_\infty}{\varepsilon^*(\omega)-\varepsilon_\infty}-1\right]^{1/a\xi}\frac{\delta^c}{B'}\frac{1}{(i\omega)^{(1/\xi-c)}}. \tag{24}$$

III. EXPERIMENTAL PART

The dielectric and mechanical measurements were done at the laboratory of N. B. Olsen in IMFUFA, Roskilde University Center, Denmark. The mechanical measurement was carried out at different temperatures using a piezoelectric transducer cell, enabling one to measure the complex shear modulus in the frequency interval from 10^{-2} Hz to 10^2 kHz. For the dielectric measurement, a HP4192A impedance analyzer was used in the same frequency interval. The experimental cell, temperature controller, and procedure to collect

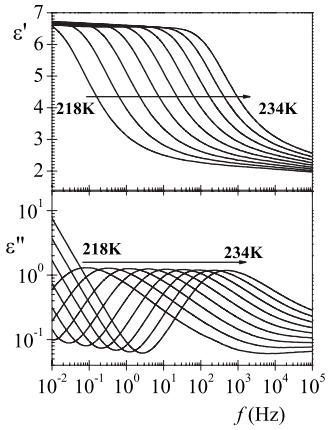

FIG. 1. Real and imaginary parts of the complex dielectric permittivity as a function of frequency at temperatures between 218 and 234 K (step 2 K).

data were described previously.[27] The glass transition temperature T_g of this glass forming liquid analyzed (DCMMS) is 220 K as previously reported.[14]

A. Experimental results

Isotherms representing the permittivity and the dielectric loss are shown at several temperatures (between 218 and 234 K, step 2 K) in Fig. 1. The loss curves at 1 Hz, display a well developed α-relaxation at temperature near the glass transition temperature. We can observe, in addition to the dipolar α relaxation, the presence of conductive contribution at high temperatures and low frequencies. Moreover, at low temperatures and high frequencies, a second dipolar process, overlapped with first seems to be present.

In Fig. 2 are represented the spectra of the real and imaginary parts of the shear modulus at different temperatures. Owing to the large half width of the isotherms representing the imaginary part of the shear modulus, we presume the presence of a secondary process overlapped to the α relaxation process in the interval of temperatures and frequencies analyzed.

B. Dielectric characterization

To proceed to do deconvolution of α and β relaxations, we start noting that a single relaxation processes corresponds

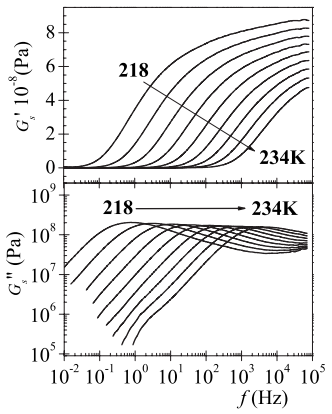

FIG. 2. Real and imaginary parts of the shear modulus as a function of frequency at temperatures between 218 and 234 K (step 2K).

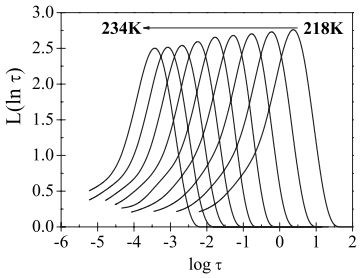

FIG. 3. Retardation spectra in the temperatures between 218 and 234 K (step 2K).

to a Dirac delta function in the time domain. This is in contrast with the broadness of these processes in the frequency domain, and for this reason, it is convenient to express the actual data in terms of the retardation time spectrum.

The complex dielectric permittivity can be expressed in terms of the retardation time spectrum by[28]

$$\hat{\varepsilon}(\omega) = \int_{-\infty}^{\infty} \frac{\Delta\varepsilon}{1+i\omega\tau} L(\ln\,\tau) d(\ln\,\tau) + \left(\frac{\sigma_0}{i\varepsilon_{\text{vac}}\omega}\right)^s + \varepsilon_\infty$$

$$\approx \sum_{k=1}^{N} \frac{\Delta\varepsilon}{1+i\omega\tau_k} L_k(\ln\,\tau) + \left(\frac{\sigma_0}{i\varepsilon_{\text{vac}}\omega}\right)^s + \varepsilon_\infty, \tag{25}$$

where τ is the retardation time, ω is the angular frequency, $\Delta\varepsilon$ is the strengths of the relaxation, $L(\ln\,\tau)$ is the retardation time distribution, σ_0 is the ionic conductivity, s is the exponent of the conductivity, ε_{vac} is the dielectric permittivity in vacuum (8.8542×10^{-12} N^{-1} m^{-2} C^2), and ε_∞ is the unrelaxed permittivity.

Retardation spectra, obtained by means of numerical procedure describe in Ref. 28, for DCMMS in the temperature window 218–234 K, are shown in Fig. 3. As we can observe, the form of the spectra indicates the presence of at least two processes, but the peaks associated with these processes mutually overlap.

The analysis of the retardation time spectra was carried out assuming that the spectra obey Havriliak–Negami (HN) empirical equation.[29] The pertinent expression for $L(\ln\,\tau)$ is given by[30]

$$L(\ln\,\tau) = \frac{1}{\pi}\frac{(\tau/\tau_{\text{HN}})^{ab}\sin b\theta}{[(\tau/\tau_{\text{HN}})^{2a} + 2(\tau/\tau_{\text{HN}})^a\cos a\pi + 1]^{b/2}},$$

$$\text{with} \quad \theta = \arctan\left(\frac{\sin a\pi}{(\tau/\tau_{\text{HN}})^a + \cos a\pi}\right) \quad \text{for} \quad \theta > 0,$$

$$\text{and} \quad \theta = \arctan\left(\frac{\sin a\pi}{(\tau/\tau_{\text{HN}})^a + \cos a\pi}\right) + \pi \quad \text{for} \quad \theta < 0 \tag{26}$$

where a and b are the shape parameters for the α relaxation, whereas τ_{HN} is a characteristic relaxation time. An additive rule for the permittivity is assumed to be valid for the overlapping of the two found processes.

For each temperature, a good fitting was only accomplished by assuming the spectrum as the result of the overlapping of the α-relaxation and one secondary relaxation.

TABLE I. Fitting HN parameters (dielectric) obtained for DCMMS using Eq. (26).

T (K)	$\Delta\varepsilon_\alpha$	a_α	b_α	$\log[\tau_{HN,\alpha}(s)]$	$\Delta\varepsilon_\beta$	a_β	b_β	$\log[\tau_{HN,\beta}(s)]$
218	3.888	0.85	0.36	0.800	0.957	0.74	1	0.155
220	3.847	0.86	0.36	0.173	1.00	0.77	1	−0.458
222	3.656	0.86	0.35	−0.352	1.060	0.75	1	−0.975
224	3.575	0.87	0.35	−0.873	1.161	0.76	1	−1.493
226	3.486	0.87	0.34	−1.350	1.210	0.76	1	−1.967
228	3.332	0.87	0.32	−1.785	1.346	0.76	1	−2.421
230	3.272	0.87	0.31	−2.193	1.379	0.76	1	−2.845
232	3.272	0.87	0.30	−2.577	1.379	0.76	1	−3.228
234	3.253	0.87	0.29	−2.936	1.379	0.76	1	−3.599
Uncertainty	±0.001	±0.01	±0.02	±0.002	±0.002	±0.02	±0.01	±0.005

The deconvolution was carried out by means of a least-squares error fitting methodology by using the methodology previously described.[31–35] The values of the HN parameters obtained are summarized in Table I. The quality of the fitting procedure is shown in the last line of Table I in terms of the general uncertainty and in Fig. 4, where as an example, the overall and the deconvoluted spectra of the α and β relaxations at 228 K are shown.

Both relaxation processes have a value of a_i $(i=\alpha,\beta)$ that slightly increases with increasing temperature. However, the b_α parameter undergoes a slight decreases with increasing temperature and the b_β parameter takes the value of 1 for all temperatures, which corresponds to the Cole–Cole symmetric function as expected for the secondary relaxations. The strengths of the relaxations were calculated by means of the following expression:

$$\Delta\varepsilon_i = \int_{-\infty}^{\infty} L_i(\ln\tau)d\ln\tau, \tag{27}$$

where the subscript i refers to the relaxation processes (α and β).

In Table I the strengths of the relaxations obtained for the temperature interval analyzed are summarized. The temperature dependence of the strengths of the processes follows the classical trends, that is, the strength of the β relaxation increases with increasing temperature, whereas the strength of the α relaxation decreases with increasing temperature.

On the other hand, the relaxation times associated with the peak maxima of the β process shows an Arrhenius-like temperature dependence, but corresponding to the α process is non-Arrhenius and present a Vogel–Fulcher–Tamman dependence.[36]

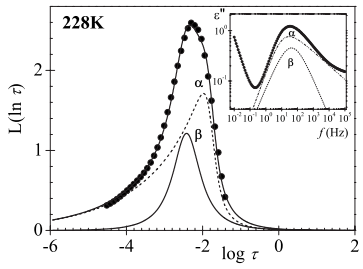

FIG. 4. Deconvolution of the retardation spectrum for DCMMS at 228 K. The comparison of the calculated dielectric loss from the spectrum (curves) and the experimental results (circles) is shown in the inset.

C. Mechanical characterization

As mentioned previously, the mechanical spectra show the overlapping of two relaxations processes (α and β). Thus, also in this case, in order to characterize and to analyze the mechanical spectra, it was necessary to split the observed relaxations into their components.

In this case, the deconvolution was carried out by using only the imaginary part of the shear modulus, also assuming additivity of the processes. In this case, the empirical HN model was also employed,[29]

$$G_s''(\omega) = \sum_{k=\alpha,\beta} \mathrm{Im}\left[\frac{G_{0,k}-G_{\infty,k}}{(1+(i\omega\tau_{s,k})^{c_k})^{d_k}}\right], \tag{28}$$

where G_0 is the relaxed shear modulus, G_∞ is the unrelaxed shear modulus, τ_s is mechanical relaxation time, and c and d are the shape parameters. For the secondary processes, the d parameter takes the value of 1.

Table II summarizes the fitting HN parameters obtained by means of a least-squares error fitting methodology by using Eq. (28). As we can see, the temperature dependence of the fitting HN parameters is similar to that one observed from dielectric results (Table I).

The precision of the fit parameters is shown in the lowest part of the Table II and, in Fig. 5, where, as an example, the overall spectrum of G_s'' and their splitting into α and β relaxations at 228 K are shown.

IV. APPLICATION OF THE INTERCONVERSION ALGORITM

A. Rotational viscosity

By using the generalization of the rotational viscosity that uses a power law with a fractional exponent proposed previously, Eq. (13), we could evaluate the rotational viscosity as a function of the HN parameters as

TABLE II. Fitting HN parameters (mechanical) obtained for DCMMS using Eq. (28).

T (K)	$G_{\infty,\alpha}$-$G_{0,\alpha}\times10^{-8}$(Pa)	c_α	d_α	$\log[\tau_{s,\alpha}(s)]$	$G_{\infty,\beta}$-$G_{0,\beta}\times10^{-8}$(Pa)	c_β	d_β	$\log[\tau_{s,\beta}(s)]$
218	8.09	0.93	0.24	0.004	1.03	0.86	1	−0.963
220	7.71	0.92	0.24	−0.602	1.14	0.77	1	−1.516
222	7.48	0.91	0.25	−1.171	1.15	0.73	1	−2.050
224	7.41	0.93	0.22	−1.656	1.17	0.73	1	−2.564
226	7.36	0.94	0.19	−2.104	1.27	0.75	1	−3.020
228	7.28	0.95	0.18	−2.550	1.31	0.74	1	−3.416
230	7.24	0.96	0.17	−2.987	1.33	0.69	1	−3.824
232	7.24	0.97	0.17	−3.370	1.33	0.67	1	−4.233
234	7.24	0.98	0.16	−3.730	1.33	0.63	1	−4.616
Uncertainty	±0.02	±0.03	±0.03	±0.004	±0.03	±0.04	±0.01	±0.005

$$A\,\eta^*_{\mathrm{rot}}(\omega)=\frac{1}{i\omega}\{[1+(i\omega\tau_{\mathrm{HN},\alpha})^{a_\alpha}]^{b_\alpha}-1\}^{1/a}. \tag{29}$$

In the last equation, surprisingly, the divergences at low frequencies disappear when the parameter a takes the same value of a_α in the HN equation (this is $a=a_\alpha$). That is, the real and imaginary rotational viscosities present a behavior that it is in agreement with the characteristics of a single relaxation band theory.[2] We can appreciate this fact in Fig. 6, where the real and imaginary parts of α rotational viscosity at different temperatures, evaluated by means of Eq. (29), are plotted as a function of the frequency.

In addition, we evaluated the modulus and phase angle of the α rotational viscosity at temperatures in the range of 218–234 K and the results are plotted in function of frequency in Fig. 7. As we can see the value of the modulus diminishes with increasing temperature as expected, whereas the phase angle shows a displacement to higher frequencies with increasing temperature.

B. Translational viscosity

According to Eq. (18), the α translational viscosity can be evaluated as a function of the HN parameters as

$$\eta^*_{\mathrm{trans}}(\omega)=\frac{G^*_{s,\alpha}-G_{0,\alpha}}{(i\omega)^{c_\alpha}}=\frac{G_{\infty,\alpha}-G_{0,\alpha}}{(i\omega)^{c_\alpha}(1+(i\omega\tau_{s,\alpha})^{c_\alpha})^{d_\alpha}}. \tag{30}$$

As the dielectric case, it also is surprise that the parameter c is the same value of c_α in the HN equation ($c=c_\alpha$).

In Fig. 8, are plotted the real and imaginary parts of the α translational viscosity evaluated by means of Eq. (30) with the HN parameters summarized in Table II. The frequency dependence of the real and imaginary translational viscosities is in agreement with the expected behavior. In the same way, the frequency dependence of the modulus and the phase angle of the translational viscosity have been evaluated and plotted in Fig. 9. As we can see, the frequency dependence of the modulus and phase angle is similar to that obtained from the rotational viscosity results.

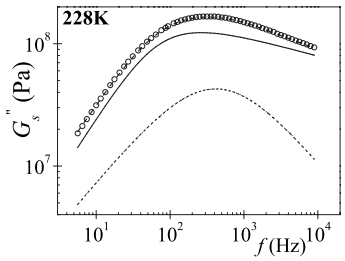

FIG. 5. Deconvoluted mechanical loss curves at 228 K. Black circles correspond to the experimental data and lines the result of fit.

C. Comparison of the rotational viscosity evaluated from dielectric measurements and from mechanical measurements

In order to verify the accuracy of the proposed model, we compared the modulus and angle phase evaluate from experimental dielectric data with those one obtained by means of mechanical experimental data through Eqs. (29) and (30). As an example, the frequency dependence of the modulus and phase angle of the rotational viscosity obtained from dielectric and mechanical experimental data, at three temperatures (218, 224, and 230 K), is shown in Fig. 10.

D. Evaluation of the dielectric permittivity from shear modulus and shear modulus from dielectric permittivity

In addition, in order to verify the accuracy of the proposed model, we compared the α dielectric permittivity ex-

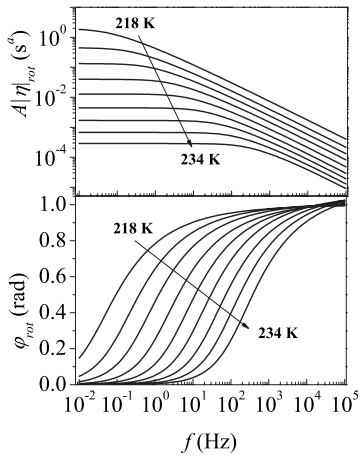

FIG. 6. Real and imaginary parts of α rotational viscosity as a function of frequency at temperatures between 218 and 234 K (step 2 K), according to Eq. (29).

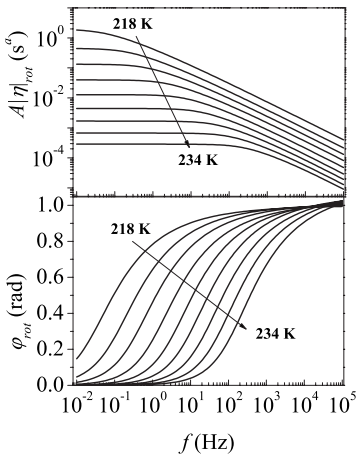

FIG. 7. Modulus and phase angle of α rotational viscosity as a function of frequency at temperatures between 218 and 234 K (step 2 K).

perimental data with those one evaluated by means of Eq. (23), i.e., from the fitting parameters of the mechanical measurements (Table II).

In Fig. 11, we plotted the results obtained at 218, 224, and 230 K. As can be seen, the values of real and imaginary permittivities evaluated from mechanical data are very similar to those directly obtained from the experimental dielectric measurements.

The calculated shear modulus [by using Eq. (24)] and the experimental data are plotted at three different temperatures (218, 224, and 230 K) and are shown in Fig. 12. In this case, the proposed model [Eq. (24)] reproduces values of the imaginary shear modulus that are more accurate than the corresponding to the real shear modulus. This fact could be related to the fact that in the fit method employed, in order to characterize the α-mechanical relaxation, only the imaginary shear modulus was used.

Table III summarizes the obtained fitting parameters of the interconversion between dielectric and mechanical data in the interval of temperatures of 218–234 at step of 2 K. According to the results, the scale factor B in Eq. (20) slightly decreases with increasing temperature. On the other

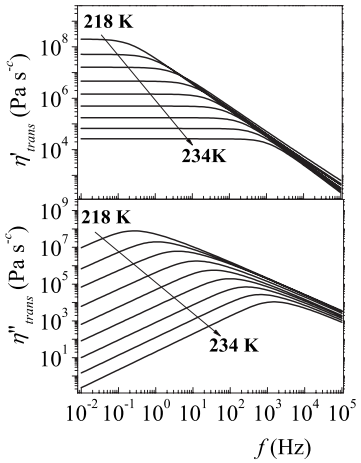

FIG. 8. Real and imaginary parts of α translational viscosity as a function of frequency at temperatures between 218 and 234 K (step 2 K), according to Eq. (30).

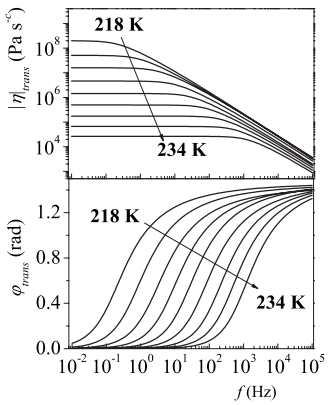

FIG. 9. Modulus and phase angle of alpha translational viscosity as a function of frequency at temperatures between 218 and 234 K (step 2 K).

hand, in the temperature range analyzed, the form factor ξ in Eq. (20) remains approximately constant. It is interesting to note that, at high frequency, the slope of the dissipative modulus is very sensitive to the value of the ξ parameter. Finally, the shift parameter δ in Eq. (20) remains constant between 218 and 232 K and at the two greatest temperatures slightly increases.

V. CONCLUSIONS

The main features of the present research can be summarized as follows:

(1) The CTRW model was used to generalize the DMB equation in order to get better results in the interconversion between dielectric and mechanical measurements. The CTRW model was applied to describe both dielectric and shear modulus. This procedure allows defining of the generalized rotational viscosity, as well as the generalized shear viscosities. Therefore, generalized rotational and translational viscosities have been calculated considering our system as a time fractal and the fluid as a non-Newtonian. In both cases the expressions for calculations employed a fractional exponent in the term $i\omega$. These fractional exponents, a (rotational) and c

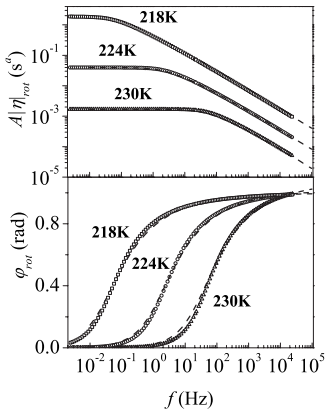

FIG. 10. Comparison of modulus and phase angle of α rotational viscosity determinate from dielectric measurement [218 K (square), 224 K (circle) and 230 K (triangle)] and from mechanical measurement, using Eqs. (20) and (29) (dash lines).

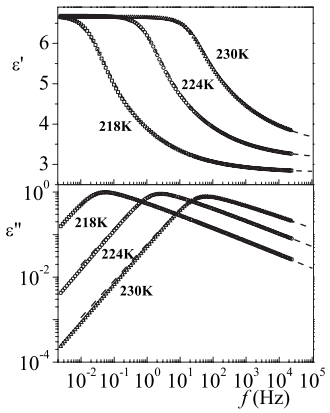

FIG. 11. Comparison of α dielectric permittivity obtained from dielectric measurement [218 K (square), 224 K (circle), and 230 K (triangle)] and from mechanical measurement, according to Eq. (23) (dash lines).

(translational), are equal to the shape parameters of the HN equations (a_α and c_α).

(2) We demonstrated that the experimental results of DCMMS shown in the experimental range of frequencies and temperatures are more than one relaxation process. In order to get that, the deconvolution of the overlapping dielectric peaks has been carried out in the time domain via the retardation spectrum. For mechanical measurements this procedure is also necessary because the overlapping of the peaks is also so severe than in the dielectric case. The obtained results for the dielectric and mechanical processes together with the values of uncertainty are reported in Tables I and II. The particular fit at 228K is shown in Figs. 4 and 5.

(3) The interconversion between dielectric and mechanical measurement for α relaxation has been carried out by using a relation between rotational and shear viscosities. Associated with this relation there are three parameters. They are related to the vertical shift (B) or scale factor to the horizontal shift (δ) and a shape factor (ξ). The vertical shift is related to the different magnitudes of dielectric and mechanical measurements. With respect to the horizontal shift δ is the inverse of the separation of the maxima of each modulus in the frequency domain. The physical interpretation of this shift is the delay in the time response to rotational and translational motions. The obtained value is about 0.24 and is constant independent of the temperature. A similar horizontal shift has been observed in previous measurements.[4] The shape factor is an exponent that takes into account the kinetic differences of both viscosities and it is related to the slope ratio of them in a logarithm plot. Their physical interpretation is related to the degree of interconversion between the shear and rotational viscosities. This interpretation was mentioned in the literature as coupling between viscosities. $\xi=1$ represents the case in which both viscosities are total coupling and $\xi=0$ is the case in which both viscosities are originated from different molecular mechanism and both viscosities are independent from each other. This parameter depends on temperature and also depends on the nature of the involved relaxation. In fact, the results obtained for the alpha relaxation interconversion ξ varies from 0.687 (218 K) to 0.721 (234 K). For the beta relaxation ξ is considered equal to zero, since the rotational viscosity is a constant, but the shear viscosity is non-Newtonian depending on the frequency. The molecular mechanisms involved in both viscosities are strictly different. The consequence of this conclusion is that there is not possible interconversion between those measurements in the case of beta relaxation.

(4) An important point is that in our proposal for the interconversion, the shape factor, is valid in the frequency domain and allows to fulfill the Kramer–Kronig relations, since this factor is equal for the real and imaginary parts of the complex rotational viscosities.

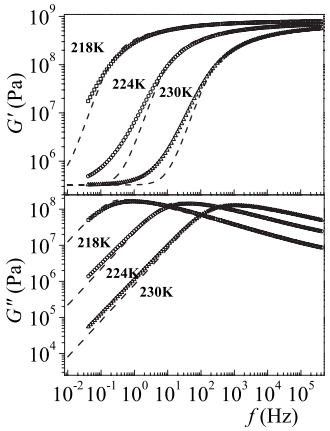

FIG. 12. Comparison of α shear modulus obtained from mechanical measurement [218 K (square), 224 K (circle), and 230 K (triangle)] and from dielectric measurement by means of Eq. (24) (dash lines).

TABLE III. Fitting parameters of the interconversion for DCMMS (the value of G_0 is taking 3.2×10^5 Pa for all temperatures).

T (K)	$\log[B([\text{Pa s}]^{\xi-1})]$	ξ	δ
218	−5.43	0.687	0.24
220	−5.82	0.711	0.24
222	−6.01	0.712	0.24
224	−6.10	0.705	0.24
226	−6.27	0.711	0.24
228	−6.48	0.725	0.24
230	−6.57	0.724	0.24
232	−6.69	0.729	0.23
234	−6.73	0.721	0.21
Uncertainty	±0.02	±0.002	±0.01

According to the results, we can conclude that the present model shows significant improvements with respect to those previously employed. Thus, in the interval of frequencies, 10^{-2}–10^{+5} Hz, the proposed interconversion model allows us to obtain more accurate results than those one obtained in the previous papers.[14] In fact, our results show that the interconversion between the two types of data is very accurate for both the modulus and phase angle of the α-rotational viscosity. However, small deviations can be appreciated in the angle phase at high temperatures and low

frequencies. The same deviations have been observed at low frequencies in the real part of the shear modulus. However, the differences between the experimental and the simulated data are of minor relevance, since it should be noted that these deviations can be due to errors propagation induced by the numerical manipulation in the interconversion of measurements by using a mathematical algorithm. Summing up, we can conclude that a high compatibility there exists between the obtained results using the proposed model and the experimental data.

ACKNOWLEDGMENTS

M.J.S., A.G.-B., and R.D.-C. gratefully acknowledge CICYT for Grant No. MAT2008-06725-C03-03. L.F.d.C. wishes to acknowledge economical support from the DGAPA-UNAM Proyecto Grant No. IN 112109 and CONACYT-SEP Grant No. C01-47070. The authors especially thank Professor Niels Boye Olsen from Roskilde Universitetcenter (Denmark) for dielectric and mechanical measurements.

[1]E. A. Dimarzio and M. Bishop, J. Chem. Phys. **60**, 3802 (1974).
[2]A. Gemant, Trans. Faraday Soc. **31**, 1582 (1935).
[3]R. Díaz-Calleja, E. Riande, and J. San Román, Polymer **32**, 2995 (1991).
[4]R. Díaz-Calleja, E. Riande, and J. San Román, J. Polym. Sci., Part B: Polym. Phys. **31**, 711 (1993).
[5]K. Niss, B. Jakobsen, and N. B. Olsen, J. Chem. Phys. **123**, 234510 (2005).
[6]P. Debye, *Polar Molecules* (Dover, New York, 1929).
[7]W. T. Coffey, Y. P. Kalmykov, and S. V. Titov, J. Chem. Phys. **116**, 6422 (2002).
[8]Y. R. Metzler and J. Klafter, Phys. Rep. **339**, 1 (2000).
[9]Y. P. Kalmykov, W. T. Coffey, D. S. F. Crothers, and S. V. Titov, Phys. Rev. E **70**, 041103 (2004).
[10]E. Barkai and R. S. Silbey, J. Phys. Chem. B **104**, 3866 (2000).
[11]R. Metzler, E. Barkai, and J. Klafter, Phys. Rev. Lett. **82**, 3563 (1999).
[12]H. Scher, M. F. Shlesinger, and J. T. Bendler, Phys. Today **44**, 26 (1991).
[13]J. C. Dyre, J. Appl. Phys. **64**, 2456 (1988).
[14]R. Díaz-Calleja, A. Garcia-Bernabé, M. J. Sanchis, and L. F. del Castillo, Phys. Rev. E **72**, 051505 (2005).
[15]R. Díaz-Calleja, L. Gargallo, and D. Radic, Polym. Int. **29**, 159 (1992).
[16]R. Díaz-Calleja, E. Saiz, E. Riande, L. Gargallo, and D. Radic, Macromolecules **26**, 3795 (1993).
[17]R. Díaz-Calleja, L. Gargallo, and D. Radic, J. Polym. Sci., Part B: Polym. Phys. **31**, 107 (1993).
[18]F. Fujara, B. Geil, H. Sillescu, and G. Fleischer, Z. Phys B: Condens. Matter **88**, 195 (1992).
[19]I. Chang, F. Fujara, B. Geil, G. Heuberger, T. Mangel, and H. Sillescu, J. Non-Cryst. Solids **172-174**, 248 (1994).
[20]S. C. Glotzer, J. Non-Cryst. Solids **274**, 342 (2000).
[21]W. Ostwald, Kolloid-Z. **36**, 99 (1925).
[22]P. J. Carreau, D. De Kee, and M. Daroux, Can. J. Chem. Eng. **57**, 135 (1979).
[23]S. G. Samko, A. A. Kilbas, and O. I. Marichev, *Fractional Integrals and Derivatives-Theory and Applications* (Gordon and Breach, New York, 1993).
[24]K. S. Cole and R. H. Cole, J. Chem. Phys. **9**, 341 (1941).
[25]E. Riande and R. Díaz-Calleja, *Electrical Properties of Polymers* (Dekker, New York, 2004).
[26]S. C. Glotzer, V. N. Novikov, and T. B. Schoder, J. Chem. Phys. **112**, 509 (2000).
[27]T. Christensen and N. B. Olsen, Rev. Sci. Instrum. **66**, 5019 (1995).
[28]G. Domínguez-Espinosa, D. Ginestar, M. J. Sanchis, R. Díaz-Calleja, and E. Riande, J. Chem. Phys. **129**, 104513 (2008).
[29]S. Havriliak and S. Negami, Polymer **8**, 161 (1967); J. Polym. Sci., Part C-Polym. Symp. **14**, 99 (1966).
[30]D. Gómez, A. Alegría, A. Arbe, and J. Colmenero, Macromolecules **34**, 503 (2001).
[31]G. Domínguez-Espinosa, R. Díaz-Calleja, E. Riande, L. Gargallo, and D. Radic, Macromolecules **39**, 3071 (2006).
[32]G. Domínguez-Espinosa, R. Díaz-Calleja, and E. Riande, Macromolecules **39**, 5043 (2006).
[33]M. J. Sanchis, G. Domínguez-Espinosa, R. Díaz-Calleja, J. Guzmán, and E. Riande, J. Chem. Phys. **129**, 054903 (2008).
[34]R. Díaz-Calleja, G. Domínguez-Espinosa, and E. Riande, J. Non-Cryst. Solids **353**, 719 (2007).
[35]A. Garcia-Bernabé, G. Domínguez-Espinosa, R. Díaz-Calleja, E. Riande, and R. Haag, J. Chem. Phys. **127**, 124904 (2007).
[36]H. Vogel, Phys. Z. **22**, 645 (1921); G. S. Fulcher, J. Am. Ceram. Soc. **8**, 339 (1925); G. Tammann and W. Hesse, J. Soc. Glass Technol. **9**, 166 (1926).